Hot-phonon effects and interband relaxation processes in photoexcited GaAs quantum wells

R. P. Joshi and D. K. Ferry
Center for Solid State Electronics Research, Arizona State University, Tempe, Arizona 85287-6206
(Received 29 April 1988)

We present a theoretical study of the thermalization process of laser-excited, electron-hole plasmas in quantum wells. In particular, the long-time behavior of the light holes is investigated to determine their effect and the role played by the nonequilibrium phonons on the relaxation dynamics. We find that phonon reabsorption by the light holes can result in a significant heating of this population. The consequent retardation in the cooling is further augmented by the bottleneck effect arising out of energy-threshold limitations for the inter- and intraband phonon-emission processes. It is possible to obtain light-hole temperatures exceeding those of the electrons for some values of the lattice temperature and well width. Our results compare favorably with recent experimental observations.

I. INTRODUCTION

The cooling of hot, photoexcited carriers in quantum-well structures has been extensively investigated, both theoretically[1-4] and experimentally,[5-7] in recent years. Theoretical results for the carrier cooling, phonon distribution functions,[8,9] and energy-loss rates[10,11] have been obtained using various approaches. In most cases it has been implicitly assumed that the carriers occupy only the lowest subbands. Though this is a reasonable approximation at low carrier densities and colder temperatures, it is almost always violated if the well widths are not extremely short. Even if the quantum wells were not too large, the contributions from both the light and heavy holes might become important because of their larger effective mass.

It is only recently that experiments have been performed to observe the dynamics of carriers lying in the higher bands. Nuss *et al.*[12] have developed a technique to measure the transient mobility of the carriers on a fast time scale. Carrier depopulation rates and interband relaxation times have also been obtained using infrared bleaching techniques.[13] The time evolution of both the light-hole and electron temperatures has been experimentally determined[14] for a few cases. These experiments collectively indicate that cooling times for interband processes are of the order of several hundred picoseconds and depend on the width of the quantum wells.[15] Tang *et al.*[16] had earlier obtained experimental evidence of a direct relation between the cooling times and carrier densities.

The results from analytical simulations based on the lowest-subband approximation,[16,17] on the other hand, have not been able to explain the subtle aspects seen experimentally. These simulations indicate that screening is not very strong in two-dimensional systems and that the relaxation times are relatively short. These discrepancies may stem from neglecting the light-hole band, and we have shown previously that it is important to include the plasmon-phonon interactions complete with screening.[18] In order to ascertain the influence of the higher subbands and to make a comparison with recently published experimental data, we model the carrier thermalization using a many-band analytical approach.

As a first step towards a complete multisubband simulation, we include directly the light holes. The decision to use two hole bands rather than a pair of electron subbands, was based on the following considerations. First, because of their higher masses, the hole interband separation is much less than that of the electron subbands. As a result, there is a greater contribution to the carrier population from the light holes than from higher-lying electron subbands. This enhancement in the carrier density is important since it not only affects the cooling rates, but also alters the nonequilibrium phonon dynamics. Secondly, the large difference between the effective masses of the light and heavy holes makes it impossible for the more energetic light holes to relax via interband processes even for band separations less than the phonon energies. This creates a bottleneck effect, making the light-hole cooling rate considerably slower. This bottleneck effect is easily varied by changing the well width. Finally, experimental results on the cooling of light holes on long time scales are already available,[14] and indicate the presence of many of these subtle variations. It is therefore easier to compare the results of the theoretical simulation with experimental data.

In this paper we present the results of a theoretical calculation for the relaxation of photoexcited electron-hole plasmas in quantum-well structures. An analytical approach has been used to model the thermalization process. One electron and two hole bands have been used in the calculations. The various intercarrier interactions, as well as the relevant Fröhlich carrier-phonon couplings, have been included self-consistently. The carriers are quasi-two-dimensional in nature, while the phonons have been assumed to be bulklike, though more rigorous approaches of including their two-dimensional nature exist.[3,17] The focus is primarily on the importance of the light-hole band, and hence a detailed calculation of the

various modes that can exist in quantum wells has not been performed. The screening of all the Coulombic interactions has been incorporated self-consistently within the random-phase approximation. Finally, the effect of the amplification of both the TO and LO modes due to the rapid, initial energy relaxation by the carriers has also been considered. The results indicate that this phonon amplification contributes significantly to the oscillations of the light-hole temperature with respect to that of the electrons. Moreover, these oscillations are strongly dependent on the carrier-recombination rates.

II. THE THEORETICAL APPROACH

As discussed above, the time scale of interest here extends to several hundred picoseconds. It is therefore quite reasonable to use a quasiequilibrium Fermi-Dirac distribution for the various carriers. The use of these quasiequilibrium forms for the nonequilibrium carriers has an old basis[19] and depends on microinteractions among the carriers to establish a quasiequilibrium distribution.[20] These microinteractions are primarily the intraband carrier-carrier scattering processes which quickly thermalize each constituent species to a common, local temperature. The time scales involved in such internal relaxation are well below a picosecond, as has been demonstrated experimentally from anti-Stokes luminescence measurements[21] and also by Monte Carlo simulations.[22] The approach of characterizing each carrier species by a time-evolving, heated Fermi-Dirac distribution is, therefore, well justified in the present context.

The quasiequilibrium Fermi-Dirac distribution for the various carriers is determined self-consistently at each time step by solving both the energy- and the particle-balance equations. Thus,

$$E_{Ti}(t)=\int_0^\infty E_i f(E_{Fi},T_i,t)D_i(E)dE \tag{1a}$$

and

$$n_i(t)=\int_0^\infty f(E_{Fi},T_i,t)D_i(E)dE \ , \tag{1b}$$

where $E_{Ti}(t)$ is the total energy, E_{Fi} the quasi-Fermi-level, and T_i the effective temperature for the ith carrier type at a given time. The total energies $E_{Ti}(t)$ and the carrier numbers $n_i(t)$ given in Eq. (1) are dynamic variables, changing in time because of the input from the laser pump, the interband thermalization, and the carrier-phonon energy exchange. Their time dependence is governed by the following set of equations for each carrier type:

$$\frac{\partial E^i}{\partial t}=\sum_{\text{ph}} R_{i\text{-ph}}+\sum_j R_{i\text{-}j}+R_{\text{laser}}-R_{\text{recom}} \tag{2a}$$

and

$$\frac{\partial n^i}{\partial t}=G_{\text{laser}}(t)+\sum_j T_{i\text{-}j}-T_{\text{recom}} \ . \tag{2b}$$

In the above equations, $R_{i\text{-ph}}$ represents the energy gain from the phonons, $R_{i\text{-}j}$ is due to interband carrier exchange, R_{laser} is the rate of energy input from the laser, R_{recom} is the loss rate due to recombination processes, G_{laser} is the laser electron-hole–generation rate, and $T_{i\text{-}j}$ is the interband carrier transfer rate.

The laser-pulse shape was taken to be an hyperbolic secant with the carrier generation rate $G(t)$ given by

$$G_{\text{laser}}(t)=B(t)N_{\text{tot}}\text{sech}^2[K(t-t_p/2)] \ , \tag{3}$$

where K and t_p are suitable constants related to the pulse width, N_{total} is the total number of electron-hole pairs generated, and $B(t)$ is the band-filling factor. This functional form for the pulse shape is in accord with results obtained by curve fitting experimental data. Finally, the band-filling factor $B(t)$ is given by the usual expression,

$$B(t)=1-f_e(t)-f_h(t) \ . \tag{4}$$

The energy-transfer rate $R_{i\text{-ph}}$ between the carriers and the lattice through phonon emission and absorption is given by

$$R_{i\text{-ph}}=\sum_j \hbar\omega_j[W_j^e(t)-W_j^a(t)] \ , \tag{5}$$

where the index j runs over all the possible phonon modes. In the GaAs-$Al_xGa_{1-x}As$ quantum-well structures, the electrons couple to the LO phonons through the polar-optical interaction and to the LA and TA modes through the acoustic deformation potential and piezoelectric coupling. The holes, in addition to being coupled with the LO and acoustic modes, also couple to the TO modes via the optical deformation potential.[23]

The expressions for $W_j(t)$ were obtained using the usual Fermi golden-rule–type calculations. Thus,

$$W_j^{e,a}(t)=\frac{2\pi}{\hbar}S_j(t)\delta(E)(N_j+\tfrac{1}{2}\pm\tfrac{1}{2}) \ , \tag{6}$$

with

$$S_j(t)=\int S_j^{3\text{D}}(t)F\,dq_\parallel \ .$$

In the above equations, $S_j^{3\text{D}}$ is the corresponding three-dimensional (3D) matrix element, while F is given by

$$F=\int dq_z I_{mn}(q_z) \ , \tag{7a}$$

with

$$I_{mn}=\left|\int_0^{L_z}\Psi_n^*(r)\Psi_m(r)e^{iq_z z}dz\right|^2 \ . \tag{7b}$$

The electronic part of the wave function, $\Psi_n(r)$, has the following form:

$$\Psi_n(r)=e^{ik_\parallel x_\parallel}\phi_n(z) \ , \tag{8}$$

$\phi_n(z)$ being the solution of the 1D Schrödinger equation,

$$(\hbar^2/2m)\frac{d^2\phi_n(z)}{d^2z}+V_{\text{eff}}(z)\phi_n(z)=E_n\phi_n(z) \ . \tag{9}$$

In order to keep the problem simple and analytically solvable, the exchange-correlation potential was not included in V_{eff}. Furthermore, band-bending effects were neglected and V_{eff} was taken to be a finite, rectangular potential. The ratio of the depths of the conduction- and

valence-band wells was chosen to be 68:32, in accord with recent experimental findings.[24]

The coupling between the carriers and the phonons drives the phonon modes out of equilibrium because of the net phonon emission during the relaxation process.[25] We include this nonequilibrium phonon effect and explicitly determine the time evolution of the phonon distribution by the Boltzmann equation. Since the phonon-phonon interaction is quite complicated and involves a series of anharmonic terms, we have chosen to describe the phonon-phonon decay process by an effective, single-mode relaxation-time constant τ_L. The use of this relaxation-time approximation seems to work rather well in describing the net phonon decay rate. As we show elsewhere,[26] a time constant of $\tau_L = 7.75$ ps fits the Raman-scattering data extremely well at low temperatures. Under this relaxation-time approximation then, the phonon Boltzmann equation, for the phonon number $N(q,t)$, becomes

$$\frac{\delta N(q,t)}{\delta t} = \sum_c \frac{\delta N(q,t)}{\delta t}\bigg|_c - \frac{N(q,t)-N^0}{\tau_L} , \tag{10}$$

where N^0 is the equilibrium phonon occupation number, and the summation runs over all couplings of the carrier with a particular phonon mode. In our case, we consider both the LO and TO modes. The first term on the right-hand side of Eq. (10), representing the electronic contribution to the phonon buildup, can be calculated in terms of the carrier-phonon–interaction rates. Thus, neglecting quantum effects and using a Fermi golden-rule approach, the rate is given by

$$\frac{\delta N(q,t)}{\delta t}\bigg|_c = \frac{2\pi}{\hbar}\sum_k \{ |FS_{3D}^{E,c}(q)|^2 [N(q,t)+1] f_c(k)[1-f_c(k-q)]\delta(E) - |FS_{3D}^{A,c}(q)|^2 N(q,t) f_c(k)[1-f_c(k+q)]\delta(E)\} .$$

This first-order equation for the phonon modes can be easily solved, leading to the following solution:

$$N(q,t) = \exp\left[\int_0^t A(t')dt'\right] \times \left[\int_0^t B(t')\exp\left[-\int_0^{t'} A(t'')dt''\right]dt' + N^0\right] , \tag{11}$$

where

$$A = W^E - W^A - \frac{1}{\tau_L} ,$$

$$B = W^E + \frac{N^0}{t_L} ,$$

and

$$W^{E,A} = \frac{2\pi}{\hbar}\sum_k |FS_{3D}^{E,A}(q)|^2 f_c(k)[1-f_c(k-q)]\delta(E) . \tag{12}$$

The carrier-phonon interaction mentioned above has to be suitably screened because of the electrostatic nature of the coupling. We include the screening self-consistently through the longitudinal dielectric function evaluated in the random-phase approximation. The dielectric function $\epsilon(q,\omega)$ includes the polarizability of both the ions and the carrier gas with appropriate contributions from both the holes and electrons. Neglecting the contribution from the phonons, i.e., ignoring the mixing of the carrier-carrier and the carrier-phonon lines in the Feynman diagrams, the following expression for $\epsilon(q,\omega)$ results:

$$\epsilon(q,\omega) = 1 - \sum_{i,j} \frac{e^2}{2\epsilon_0\epsilon(\infty)q_\parallel} F_{ij}(q_\parallel)\Pi_{ij}(q,\omega) , \tag{13}$$

where F_{ij} and Π_{ij} are the well-known form factor and polarizability, respectively. These are mathematically given as

$$F_{ij}(q) = \int dz\, dx\, \Psi_i(z)\Psi_i^*(z)\Psi_j(x)\Psi_j^*(x)e^{-q|z-x|}$$

and in the static case

$$\Pi_{ij}(q,u) = 2\sum_k \frac{f_i(k)-f_j(k+q)}{E_i(k)-E_j(k+q)} .$$

The finite-temperature case is evaluated by using the following integral representation derived by Maldague,[27]

$$\Pi_{ij}(q,u) = \int du' G(u-u',T)\Pi_{ij}(q,u',T=0) , \tag{14}$$

with

$$G(u-u',T) = \{4kT\cosh^2[(u-u')/2kT]\}^{-1} .$$

III. RESULTS

The carrier-cooling curves for a 5-nm well width are shown in Fig. 1(a). A 3.0-ps full width at half maximum (FWHM) laser pulse, having an energy of 1.78 eV, was used. For comparison, the results for the single-hole–band calculation are also shown in Fig. 1(b). The light holes, initially, have an effective temperature between that of the electrons and the heavy holes. This is consistent with the fact that they have an intermediate effective mass. After the pulse, however, the light holes cool down rapidly until they approach a common temperature with the heavy holes. This period of rapid relaxation is dominated by interband and intraband polar-optical-phonon emission. While all types of carriers cool during this period, the light holes show a sharper decrease in their temperature because they have a higher effective mass than the electrons, are hotter than the heavy holes, and lose energy by both interband and intraband emission processes. Of the two kinds of processes,

the interband scattering rates are much lower than the intraband rates mainly for the following reason: Carriers lying higher in energy, beyond $\hbar\omega_{op}$ from the bottom of the heavy-hole minima, cannot make the transition from the light- to the heavy-hole band because of the latter's relatively flat shape. In the case of the electrons, the interband transfer would be further reduced by the lower value of the form factor F_{ij}.

The effect of the interband scattering is nonetheless evident from Fig. 2. Following an increase in the light-hole concentration during the pulse, their density begins to decrease until about 6 ps. After 6 ps their behavior is influenced by the buildup of nonequilibrium phonons, with both the LO and TO modes being driven out of equilibrium. The LO modes are excited by their coupling to both the electrons and holes via the polar-optical interactions, while the TO modes get amplified due to their coupling with the holes via the optical deformation potential.[23] The resulting time evolution of the phonon population is shown in Fig. 3(a), while the corresponding situation for a single-hole band model is given for comparison in Fig. 3(b).

A marked difference exists between the single-band and two-hole–band situations. The TO modes are more strongly amplified when the light holes are included. This is clearly due to the contribution from intersubband

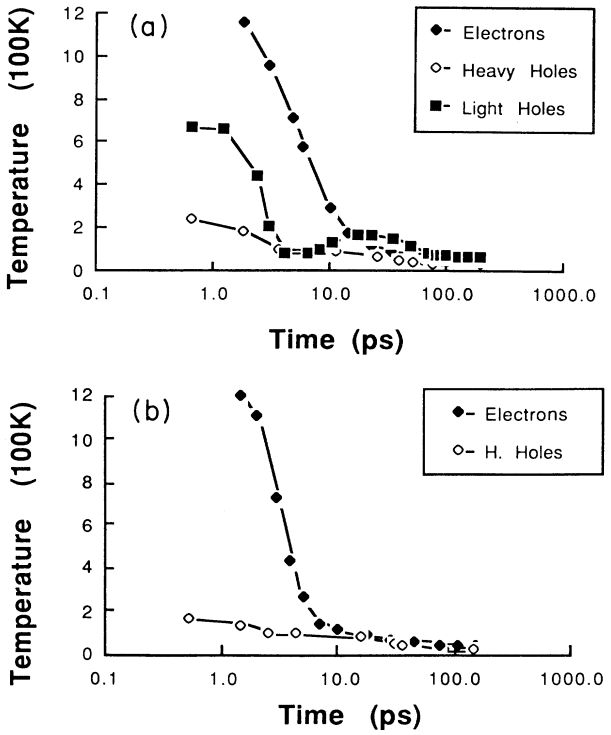

FIG. 1. (a) Time evolution of the carrier temperature for the electrons, light holes, and heavy holes for a 5-nm quantum well, and (b) time evolution of the heavy-hole and electron temperatures using a single band for each carrier type. The excitation energy was taken to be 1.78 eV from a 3-ps laser pulse. The lattice temperature was assumed to be 10 K. Both screening and the hot-phonon effects were included.

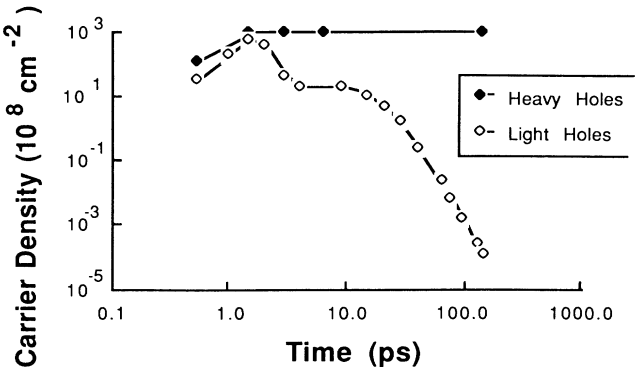

FIG. 2. The carrier concentration as a function of time for the case of Fig. 1(a). Only the heavy- and light-hole densities are shown since the time evolution of the electron density is uninteresting.

scattering processes. The LO modes, on the other hand, are not as strongly amplified as before. This is a direct consequence of enhanced screening in the two-subband situation and the effect of carrier degeneracy. Thus, the larger the number of carriers, the greater the screening of the carrier-phonon and carrier-carrier interactions, because of greater contribution from the various bands. Since the single-hole–band model neglects the photogen-

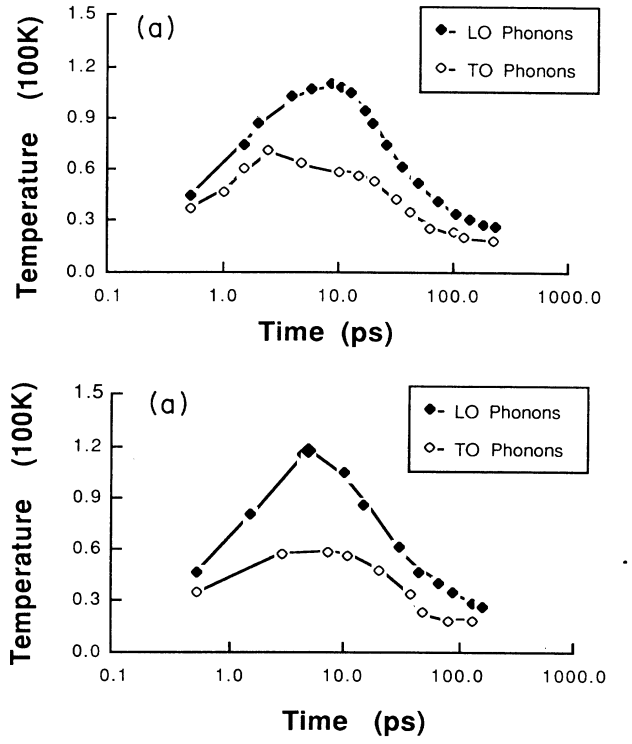

FIG. 3. (a) The effective temperature of the LO and TO modes for the three-carrier case, and (b) the time evolution of the LO- and TO-phonon temperatures using only the electron and heavy holes, so no interband scattering can arise.

eration contribution from higher-lying bands, it underestimates both the carrier number and the dielectric constant. Further, the q dependence of ϵ is such that processes involving small q values are more strongly screened. Since the electrons are more energetic than the holes, they experience a greater reduction in the electron-phonon scattering length. This reduction in the electron cooling rates was demonstrated some time ago by Shah *et al.*[6] The LO-phonon emission strength is relatively lower in this many-band model, leading to a slightly reduced hot-phonon population.

The effect of the enhanced screening is evident in the curves of Fig. 4. Only the electron temperatures have been shown for convenience. The hot-LO-phonon population obtained from the three-band model is not significantly larger than in the two-band situation, and yet the corresponding electron temperatures are much higher. This trend towards higher temperatures shown by the electrons is in keeping with the experimental results of Tang *et al.*[16] and the recent data of Ryan *et al.*[28] It is quite probable that the inclusion of higher electron subbands would lead to an even greater reduction in the cooling. Furthermore, the observed dependence of the cooling times on the carrier density would probably be explained.

The interesting behavior of the light-hole cooling is clearly seen from the plots of Figs. 5(a)–5(c). The excitation energies, pulse duration, and the photogenerated carrier densities were the same in all three cases. Figure 5(a) is merely an expanded version of Fig. 1(a) and shows the details of the simulation at longer times. The curves of Fig. 5(b) were obtained by including carrier recombination in the previous situation. Finally, the effect of changing the quantum-well width, while still incorporating the carrier-recombination processes, is shown in Fig. 5(c). The situation of Fig. 5(c) corresponds to a 4-nm well, while those of Figs. 5(a) and 5(b) are for 5-nm wells.

In all the above cases, the light holes begin to reheat at around 9 ps after nearly thermalizing with the heavy holes. This time coincides with the peak of the phonon population. It is therefore apparent that phonon reabsorption pumps energy into the carrier subsystem. Both interband and intrasubband absorption processes begin to become important. As seen from Fig. 2, the light-hole population stops decreasing during this period and levels off. This is indicative of the enhancement in the absorption-aided intersubband process, by which carriers are transferred from the heavy- to the light-hole subband. Being dependent on the phonons, this reheating is expected to be dependent on both the lattice temperature and the excitation intensity.

The cooling of the light holes takes place mostly via optical-phonon emission, since both the acoustic and the intercarrier scattering mechanisms are considerably

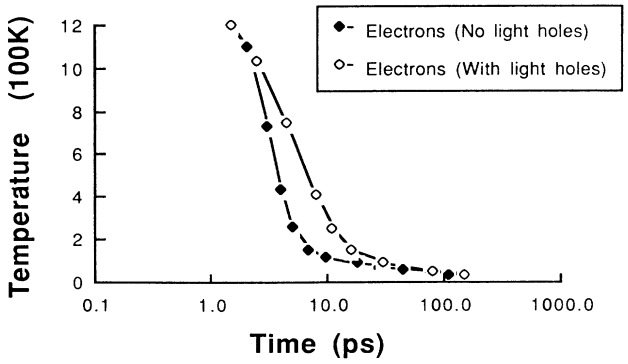

FIG. 4. Relative carrier cooling rates with and without the inclusion of the light holes. The presence of the light holes increases the density of the electrons relatively, enhancing the screening and the degeneracy effects.

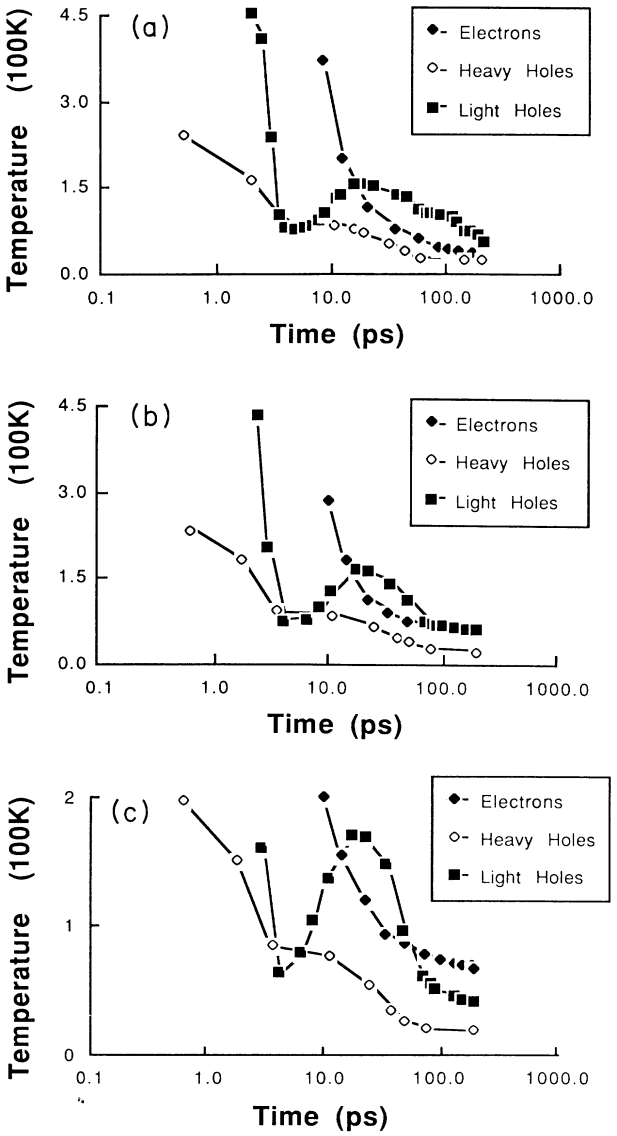

FIG. 5. (a) Expanded version of Fig. 1(a) showing the cooling behavior at longer times, (b) the effect of recombination on the carrier cooling in the three-band case (the recombination rate was taken to be about 1 ns; the light-hole temperature crosses that of the electrons at 9 ps and again at around 90 ps), and (c) the effect of narrowing the quantum-well width. A 4-nm well was used in this case as opposed to the previous value of 5 nm.

weaker. The intrasubband processes get severely limited in their energy relaxation capability once most of the light holes have energy below the threshold, $\hbar\omega_{op}$. This leaves the intersubband processes as the major channel for energy loss. This is supported by the curves of Fig. 2, which show a steady carrier change with time. Since this process, as already discussed, is not as strong as the intraband scattering, the cooling of the light holes proceeds at a much slower pace. The retardation in the cooling process is further augmented by a similar bottleneck effect on the intraband scattering at even lower temperatures. The slow interband cooling rate is in qualitative agreement with the measurements of Oberli *et al.*[29]

The role of carrier degeneracy is evidenced from the curves of Fig. 5(b). Inclusion of carrier recombination seems to have a twofold effect. First, the net rate of interband transfer to the heavy holes increases as the heavy-hole population drops with recombination. Second, recombination heating effects[30] are more pronounced for the electrons because of their large numbers and are almost negligible for the light holes. The light holes, therefore, cool a little more than do the electrons and reach lower temperatures after about 90 ps. The exact crossover seems to depend upon the recombination rate within the device. In these simulations a recombination lifetime of about 1 ns was used. Any deviation from this assumed value of the recombination rate would obviously change the crossover point. Qualitatively, however, such oscillations between the light-hole and electron temperatures and their dependence on the recombination rates are in agreement with the results obtained by Polland *et al.*[14]

The curves of Fig. 5(c) show that changing the well width effectively lowers the temperature of the light holes. This is probably due to a combination of two effects. First, the form factor associated with the scattering-rate equations increases, leading to a faster cooling. Second, the narrow well increases the relative separation between the hole bands. This enhanced separation means that the interband phonon bottleneck effect sets in much later, allowing the carrier to cool to a lower temperature. Similar dependencies of the electron cooling on the well widths have been observed experimentally by Ryan *et al.*[31]

IV. COMPARISON WITH EXPERIMENTAL DATA

A comparison of our simulation results with recent experimental data clearly brings out the importance of including the light holes in the calculations. In the present case, we have chosen to use the experimental cooling curves obtained by Ryan *et al.*[31] for undoped GaAs-$Al_xGa_{1-x}As$ quantum wells. The theoretical results agree very well with the experimental values and the cooling rates have the correct dependence on experimental parameters such as the excitation intensity, carrier densities, and well widths.

The pair of simulated electron cooling curves shown in Fig. 6 were obtained by using the same set of parameters, except that the light-hole band was entirely neglected for the lower curve. No contribution from the photogeneration process to the net electron density was therefore possible. The corresponding set of experimentally obtained data points shows an excellent fit for the many-band model. This agreement is not as good without the inclusion of the light holes. The lower carrier temperature in the absence of the light-hole band demonstrates the role of the carrier degeneracy and recombination heating. The simulation was based on the theoretical model already discussed and used a phonon lifetime of 7.75 ps at 4 K. It was not necessary to increase this lifetime in any way to account for the hotter electron temperatures.

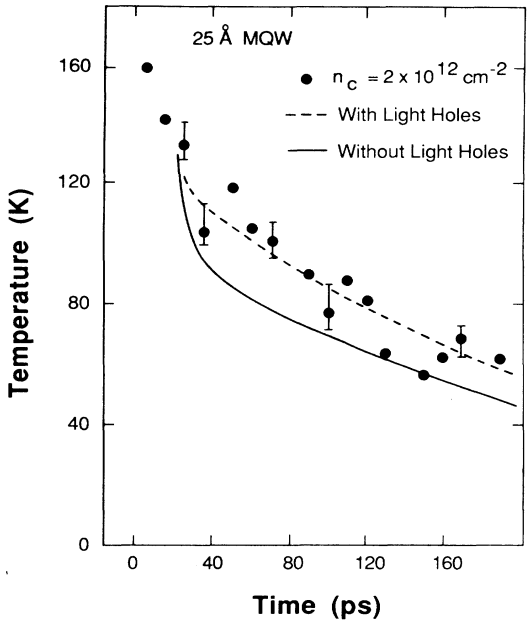

FIG. 6. The electron temperatures as a function of time obtained from two theoretical simulations. The lower curve was derived assuming a two-band model, while the upper curve included the light-hole band. The corresponding experimental data obtained by Ryan *et al.* for the same conditions is shown by scattered, unconnected data points. The quantum well was taken to be 2.5 nm wide. The excess energy of the laser pulse was set to 0.16 eV with an intensity of 2×10^{12}/cm^2. The lattice temperature was 5 K. The upper three-band curve fits the experimental results much better.

A dependence of the cooling rate on the well widths, the excitation energies, and the carrier concentration was also investigated. The results are again in good agreement with the corresponding experimentally obtained data of Ryan *et al.*[31] Figure 7(a) shows the influence of the carrier density on the cooling rate. The two curves correspond to excitation densities of 2.0×10^{12}/cm^2 and 5.0×10^{11}/cm^2. At the high densities of 2.0×10^{12}/cm^2, the shift in the energy-loss rate was particularly significant. This agrees with an earlier work which propounded the importance of Auger processes in the high-density regime.[32]

The well-width dependence is shown in Fig. 7(b) for a set of four different values. Not surprisingly, an increase in the well width decreases the cooling rate correspondingly. Finally, the effect of varying the excitation energies is seen from the curves of Fig. 7(c). A 5.6-nm quantum well was used with equal excitation densities. The

cooling for the higher-energy pulse was slightly slower in agreement with experimental data.

V. SUMMARY AND CONCLUSIONS

An analytic model was used to simulate the cooling of nonequilibrium photoexcited carriers on the picosecond time scale. The effect of the hot phonons on the relaxation process was seen to produce a relative heating of the light holes due to phonon reabsorption. Their temperatures were consequently higher than those of the electrons after a sufficient nonequilibrium phonon population had been built up. The cooling at much longer times was seen to be governed by the recombination heating and the degeneracy effects. A dependence of the electron temper-

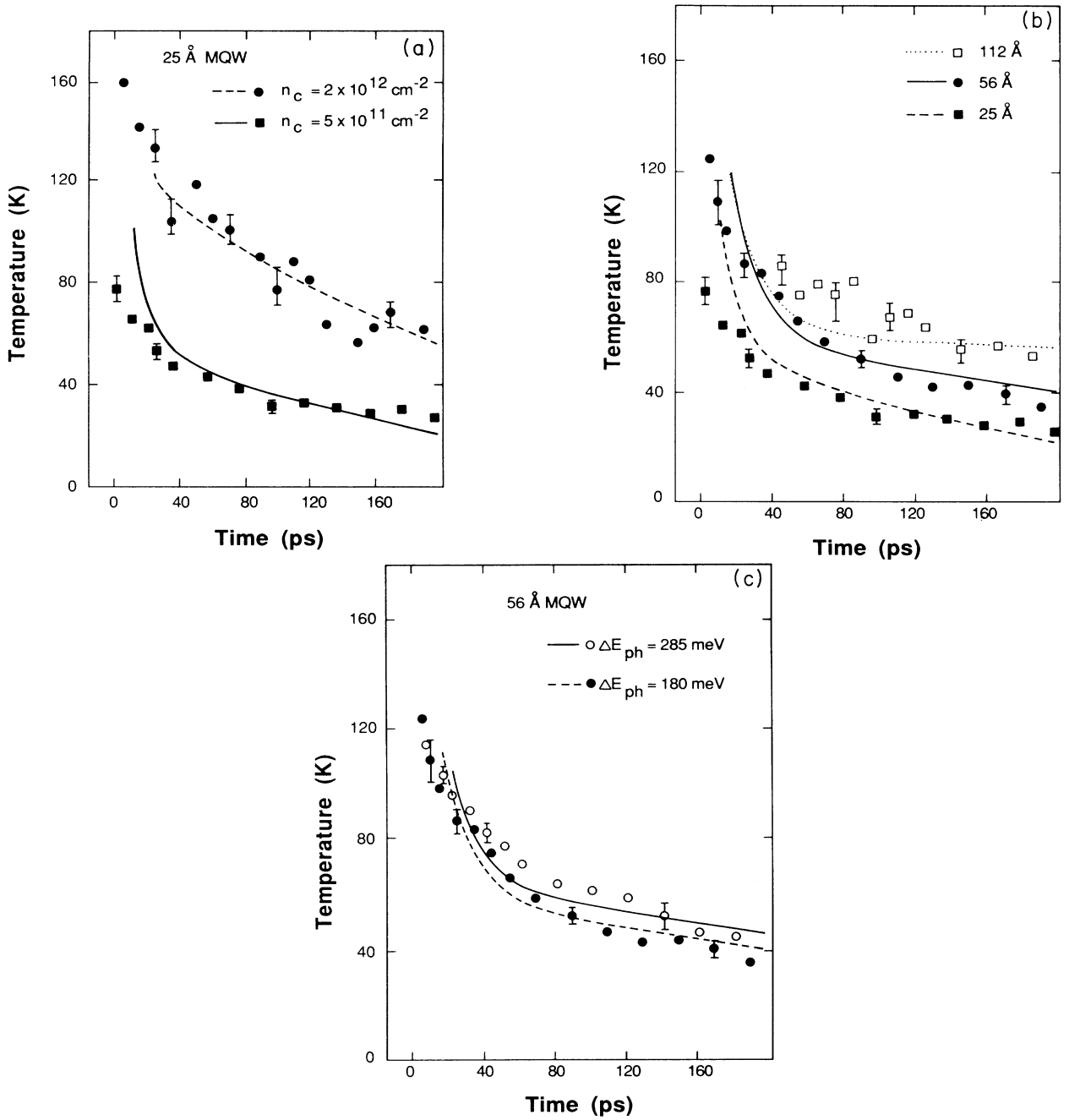

FIG. 7. Theoretical comparisons with experimental results for various values of carrier densities, quantum-well widths, and laser energies. (a) Electron cooling curves for two different photoexcitation intensities. The upper curve is for a carrier density of $2\times10^{12}/\text{cm}^2$, while the lower one is for $5\times10^{11}/\text{cm}^2$. Both simulation results match the experimental data, shown by scattered points. (b) For three different quantum-well widths. The narrower wells show a faster relaxation, again in agreement with the experimentally obtained values. (c) The comparison between theoretical data and experiments for two different photoexcitation energies. The quantum-well width was kept at 5.6 nm in both the cases.

ature on the carrier density, the photoexcitation energies, and the well width was also obtained. Furthermore, it was demonstrated that a proper inclusion of the light holes is necessary to fit the experimental data. The results obtained from the three-band model matched recent experimental data rather well.

The marked improvement obtained by including the light-hole band in a simple fashion points towards the need for detailed calculations for the multibands. This conclusion is similar to that obtained by Stanton *et al.*[33] on the basis of their Monte Carlo simulations on a femtosecond time scale. However, a more rigorous calculation for the long time scale can be quite involved, and may not be worth the effort unless one is working with wide wells or using high-energy laser pulses.

ACKNOWLEDGMENTS

We would like to thank John Ryan of Oxford University for letting us use his results prior to publication. This work has been supported by the U. S. Office of Naval Research.

[1]P. J. Price, Ann. Phys. (N.Y.) **133**, 217 (1981).
[2]B. K. Ridley, J. Phys. C **15**, 5899 (1982).
[3]W. Cai, M. C. Marchetti, and M. Lax, Phys. Rev. B **34**, 8573 (1986).
[4]P. Lugli and S. M. Goodnick, Phys. Rev. Lett. **59**, 716 (1987).
[5]C. H. Yang and S. A. Lyon, Physica B+C **134B**, 305 (1985).
[6]J. Shah, A. Pinczuk, A. C. Gossard, and W. Wiegmann, Phys. Rev. Lett. **59**, 716 (1987).
[7]W. H. Knox, C. Hirlimann, D. A. B. Miller, J. Shah, D. S. Chemla, and C. V. Shank, Phys. Rev. Lett. **56**, 1191 (1986).
[8]W. Pötz and P. Kocevar, Phys. Rev. B **28**, 7040 (1980).
[9]P. Lugli, Solid State Electron. **31**, 667 (1988).
[10]R. A. Hopfel, J. Shah, and A. C. Gossard, Phys. Rev. Lett. **56**, 765 (1986).
[11]S. Das Sarma, J. K. Jain, and R. Jalabert, Phys. Rev. B **37**, 1228 (1988).
[12]M. C. Nuss, D. H. Auston, and F. Capasso, Phys. Rev. Lett. **58**, 2355 (1987).
[13]A. Seilmeier, H. J. Hübner, G. Abstreiter, G. Weimann, and W. Schlapp, Phys. Rev. Lett. **59**, 1345 (1987).
[14]H. J. Polland, W. W. Rühle, J. Kuhl, F. Ploog, K. Fujiwara, and T. Nakayama, Phys. Rev. B **35**, 8273 (1987).
[15]M. Tatham, R. A. Taylor, J. F. Ryan, W. I. Wang, and C. T. Foxon, Solid State Electron. **31**, 459 (1988).
[16]Z. Y. Xu and C. L. Tang, Appl. Phys. Lett. **44**, 692 (1984).
[17]M. C. Marchetti and W. Pötz, J. Vac. Sci. Technol. **6**, 1341 (1988).
[18]R. P. Joshi and D. K. Ferry (unpublished).
[19]D. N. Zubarev, *Nonequilibrium Statistical Mechanics* (Consultants Bureau, New York, 1974).
[20]N. N. Bogoliubov, *Problemi dinam. teorii u stat. Fiz.* (Mir, Moscow, 1946).
[21]J. A. Kash, J. C. Tsang, and J. M. Hvam, Phys. Rev. Lett. **54**, 2151 (1985).
[22]M. A. Osman and D. K. Ferry, Phys. Rev. B **36**, 6018 (1987).
[23]M. Pugnet, J. Collet, and A. Cornet, Solid State Commun. **38**, 531 (1981).
[24]D. J. Wolford, T. F. Kuech, J. A. Bradley, M. Jaros, M. A. Gell, and D. Ninno, J. Vac. Sci. Technol. B **4**, 1043 (1986).
[25]P. Kocevar, J. Phys. C **5**, 3349 (1972).
[26]K. T. Tsen, R. P. Joshi, and D. K. Ferry (unpublished).
[27]P. F. Maldague, Surf. Sci. **73**, 296 (1978).
[28]D. J. Westland, J. F. Ryan, M. D. Scott, J. I. Davies, and J. R. Riffat, Solid State Electron. **31**, 459 (1988).
[29]D. Y. Oberli, D. R. Wake, M. V. Klein, J. Klem, T. Henderson, and H. Morkoç, Phys. Rev. Lett. **59**, 696 (1987).
[30]D. Bimberg and J. Mycielski, J. Phys. C **19**, 2363 (1986).
[31]J. F. Ryan, M. Tatham, D. J. Westland, C. T. Foxon, M. D. Scott, and W. I. Wang, Proc. SPIE 942 (1988).
[32]H. Lobentanzer, H. J. Polland, W. W. Rühle, W. Stolz, and K. Ploog, Appl. Phys. Lett. **51**, 673 (1987).
[33]C. J. Stanton, D. W. Bailey, K. Hess, and Y. C. Chang, Phys. Rev. B **37**, 6575 (1988).